

Relationships between greenhouse gas production and landscape position during short-term permafrost thaw under anaerobic conditions in the Lena Delta

Mélissa Laurent¹, Matthias Fuchs¹, Tanja Herbst¹, Alexandra Runge¹, Susanne Liebner^{2,3}, Claire C. Treat¹

¹Alfred Wegener Institute Helmholtz Centre for Polar and Marine Research, Potsdam, Germany

²GFZ German Research Centre for Geosciences, Section Geomicrobiology, Potsdam, Germany

³University of Potsdam, Institute for Biochemistry and Biology, Potsdam, Germany

Correspondence to: Mélissa Laurent (melissa.laurent@awi.de)

Field Code Changed

Abstract. Soils in the permafrost region have acted as carbon sinks for thousands of years. As a result of global warming, permafrost soils are thawing and will potentially release greenhouse gases (GHGs) such as methane (CH₄) and carbon dioxide (CO₂). However, small scale spatial heterogeneities of GHG production have been neglected in previous incubation studies. Here, we used an anaerobic incubation experiment to simulate permafrost thaw along a transect from upland Yedoma to floodplain in Kurungnakh Island. Potential CO₂ and CH₄ production were measured during incubation of active layer and permafrost soils at 4 °C and 20°C, first for 60 days (approximate length of growing season), and then continuing for one year. An assessment of methanogen abundance was performed in parallel for the first 60 days. Yedoma samples from upland and slope cores remained in a lag phase during the growing season simulation, while those located in the floodplain showed high production of CH₄ ($6.5 \times 10^3 \mu\text{g CH}_4 \mu\text{g CH}_4\text{-C gCg}^{-1} \text{C}$) and CO₂ ($6.9 \times 10^3 \mu\text{g CO}_2 \mu\text{g CO}_2\text{-C gCg}^{-1} \text{C}$) at 20°C. The Yedoma samples from the permafrost layer started producing CH₄ after six months of incubation. We conclude that landscape position is a key factor triggering CH₄ production during the growing season time in Kurungnakh Island.

Formatted: Superscript

Formatted: Superscript

Summary. Climate change is causing increasing temperatures and permafrost thaw, which might lead to increases in the release of the greenhouse gases CO₂ and CH₄. In this study, we investigated the effect of different parameters (temperature, landscape position) on the production of these gases during a one-year permafrost thaw experiment. For very similar carbon and nitrogen contents, our results show a strong heterogeneity in CH₄ production, as well as in microbial abundance. According to our study, these differences are mainly due to the landscape position and the hydrological conditions established as a result of the topography.

1 Introduction

For the past decades, scientists have warned about the effects of global climate change (IPCC 2021, IPCC 2021). The effects of this warming will be pronounced in the polar regions where the air temperature increase in the past fifty years is already three times higher than the increase in global average during the same period (AMAP, 2021; Rantanen et al., 2022). This particularly affects soils in northern high latitude permafrost regions, which cover 14.6% of the Northern Hemisphere (Obu et al., 2019) and contain 1300 Pg of organic carbon (C) (Hugelius et al., 2014a). A majority of this C (822 Pg) is stored in permafrost (Hugelius et al., 2014b) (Hugelius et al., 2014b), which is defined as ground where the temperature remains at or below 0 °C for more than two consecutive years (Washburn, 1973) (Washburn, 1973). Due to low temperatures, the organic matter (OM) stored in permafrost soils is characterized by low decomposition rate (Davidson and Janssens, 2006). However, during summer, the upper part of the permafrost affected soils thaws (active layer) and allows OM decomposition (Lee et al., 2012). With climate change, permafrost thaw will likely increase and lead to higher OM decomposition rates, releasing greenhouse gases (GHGs), like carbon dioxide (CO₂), and methane (CH₄) (Wagner et al., 2007; Schuur et al., 2015;

Knoblauch et al., 2018). This turnover might lead to the transformation of Arctic soils from C sinks to C sources (Koven et al., 2011; Dean et al., 2018; Lara et al., 2019).

Carbon emissions, and mainly CH₄ emissions greatly vary across Arctic, and especially within small scales (Treat et al., 2018; Lara et al., 2019; Elder et al., 2020). Treat et al. (2018) showed that C flux variability was strongly associated with specific landscape types due to differences in soil moisture and site drainage in uplands and wetlands that also controlled vegetation communities, which we are referring to here as landscape position. Landscape change due to permafrost thaw is also highly affected by landscape position: low-lying ice-rich areas can become waterlogged following permafrost thaw, while higher areas can be drained by water run-off (Osterkamp et al., 2009; Liljedahl et al., 2016). The water-logged areas like thermokarst lakes, or wetlands have been identified as CH₄ emissions hotspots (Olefeldt et al., 2013; Treat et al., 2018b; Kuhn et al., 2021) because of the anaerobic conditions that favour methanogen communities (Conrad, 2002; Yavitt et al., 2006). On the other hand, well-drained sites, such as upland tundra, have the capacity to offset CH₄ emissions by acting as CH₄ sinks due to net oxidation in the surface soil layer (Juncher Jørgensen et al., 2015; Treat et al., 2018). Hence, after permafrost thaw, the redox conditions, established/determined by the landscape position, lead to different microbial communities and ultimately different CH₄ emissions (McCalley et al., 2014).

To quantify CH₄ and CO₂ production and to understand C turnover from thawing permafrost, numerous incubation studies have been carried out (Lee et al., 2012; Knoblauch et al., 2018; Walz et al., 2018; Holm et al., 2020). Studies have shown that C decomposition depends on several factors, such as organic C quantity, OM quality, temperature, and oxygen availability in the soil (Ganzert et al., 2007; Lee et al., 2012; Schädel et al., 2014; Treat et al., 2015; Knoblauch et al., 2018). Additionally, in addition, Treat et al. (2015) highlighted that CH₄ production differences were partly explained by the landscape position, with differences seen between uplands, wetlands, floodplain soils, lowlands, and drained lake basins. For incubation under aerobic conditions, Kuhry et al. (2020) demonstrated that landscape types based on soil type (peaty wetlands, mineral soils) and the origin of the deposits (peat deposits, alluvial deposits) gave a good estimation of SOM lability, and therefore explained differences in CO₂ production better than using only the %C, which is a commonly used metric for C quality across incubation studies (Treat et al., 2015). However, few studies have specifically focused on how the landscape position affects CO₂ and CH₄ production under anaerobic conditions, and whether landscape position is a good indicator of CO₂ and CH₄ production under anaerobic conditions as might be expected from field observations of CO₂ and CH₄ fluxes (Treat et al., 2018; Elder et al., 2020).

Besides landscape position, climate change affects the environmental factors in the study region, it modifies weather conditions and plays a key role in controlling rain events (frequency and intensity) (Callaghan et al., 2010; Tabari, 2020; Wang et al., 2021; Fewster et al., 2022). During the past 60 years, the precipitation in Siberia has increased by 2.6 mm/decade over the year Wang et al., (2021). This finding leads likely to wetter conditions during the growing season in Siberia, and therefore, soil moisture increase/increases. Changes in soil moisture will impact vegetation cover, and soil redox conditions. Increasing precipitation and warming will also lead to deepening of the active layer (Zhu et al., 2017; Douglas et al., 2020), hence, release bioavailable C from the upper part of the permafrost layers. Waldrop et al. (2010) identified more labile C in shallow permafrost than in the active layer, which fuelled more CO₂ production in an incubation experiment. On the other hand, other incubation experiments showed higher C turnover and more CO₂ production in the active layer than in the permafrost (Walz et al., 2017; Faucherre et al., 2018). Regarding CH₄ production, incubation studies tend to show higher CH₄ production in the active layer than in shallow permafrost (Treat et al., 2015), but some studies also measured the opposite behaviour among their samples (Wagner et al., 2007; Waldrop et al., 2010). Therefore, it is still unclear how much CO₂ and CH₄ can be produced from shallow permafrost. Furthermore, high CH₄ production heterogeneity as well as long lag time have been measured with samples from Kurungnakh Island, Lena Delta, Russia (Knoblauch et al., 2013, 2018). Hence, the question remains whether the methanogen communities will have the time to activate/become active during the short growing season (60 days) under anaerobic condition, remains.

The aim of this study ~~is was~~ to simulate permafrost thaw under wet growing season conditions across different landscape units in the Lena Delta, ~~Siberia~~ and measure CO₂ and CH₄ production. Here, we incubated upland Yedoma and adjacent lowland floodplain samples under anaerobic conditions, and focused on the relationships between GHG production and microbial abundance shifts following short-term (60 days, growing season length) and longer-term (1 year) permafrost thaw. The objectives of the study were to: (1) quantify CH₄ and CO₂ production over one year under anaerobic incubation; (2) establish relationships between CH₄ and CO₂ production and methanogen abundances; and (3) characterize the role of the landscape position on gas production in thawed permafrost soils during a growing-season time frame.

2 Materials and methods

2.1 Site description and sampling

Soil samples were collected in August 2018 on Kurungnakh Island (72.333° N, 126.283° E), Lena Delta, Siberia (Figure 1). Kurungnakh Island is located in the continuous permafrost zone and is an erosional remnant of Late Pleistocene deposits, characterized by ice- and organic-rich sediments (Grigoriev, 1993; Schwamborn et al., 2002); (Grigoriev, 1993; Schwamborn et al., 2002); most of the island is composed of fluvial sandy sediments and Yedoma Ice Complex (IC) deposits. The IC is made up of ice-saturated sediments (65% to 90%), composed of cryoturbated silty sands and peaty deposits of Holocene origin (Schwamborn et al., 2002; Schirrmeister et al., 2011, 2013); (Schwamborn et al., 2002; Schirrmeister et al., 2011, 2013). Sediments from the Yedoma IC contain on average 3% total organic carbon (TOC) (Strauss et al., 2013a); (Strauss et al., 2013a), however, IC sediments can include organic-rich layers, with TOC content reaching more than 20% in layers contained within the ice complex sediments (e.g. buried peat horizons, Andreev et al., 2009). Kurungnakh Island is characterised by thermokarst lakes and wetlands due to thermo-erosional activity (Morgenstern et al., 2021); (Morgenstern et al., 2021). Samples were also collected in the young Kurungnakh Island floodplain area. The young and active floodplains in the Lena River Delta are of Holocene deltaic origin and are composed of stratified middle to fine sands and silts with layers of autochthonous peat and allochthonous OM (Schwamborn et al., 2002; Boike et al., 2013).

The soil sampling was carried out in two stages. First, the active layer was extracted using a spade, and active layer samples were collected using a fixed volume cylinder (250 cm³). Then, permafrost soil cores were sampled to a depth of one meter below surface, by drilling with a modified snow ice and permafrost (SPIRE) auger (Jon Holmgren's Machine Shop, Alaska, USA). For this study, three cores were selected, two were from the Yedoma deposits (P15 and P16) and one belonged to a floodplain area (P17). The three coring locations were on a well-drained upland soil (P15; Supplementary Fig 1), on a north-eastern facing slope (P16), and on a floodplain (P17; Figure 1). The floodplain samples were taken in the highest part of the floodplain, 5 m above the Lena River water level.

These cores were chosen on the basis of geographical proximity to each other, landscape position, moisture gradient, and ice composition. The three cores had an organic layer ranging between 3 to 7 cm (Yedoma and floodplain, respectively). Below this organic surface layer, the soil cores were identified as mineral soil. The permafrost layers from the Yedoma cores were ice-rich, while no visible ice structure was seen for the floodplain core (Table 1).

Cores were described and subsampled in the field. Detailed core descriptions are presented in Table 1 and Supplementary Table 1. For the purpose of our study, we chose two samples from each core, one from the active layer and one from the frozen layer (above 1 m depth to simulate shallow permafrost thaw; Supplementary Table 1). Care was taken not to select samples from the top of the active layer in order to avoid the top organic layers. Cores were subsampled in a climate chamber at -4 °C with a hammer and a chisel instead of a saw, to limit contamination.

Formatted: Font: +Body (Times New Roman)

Field Code Changed

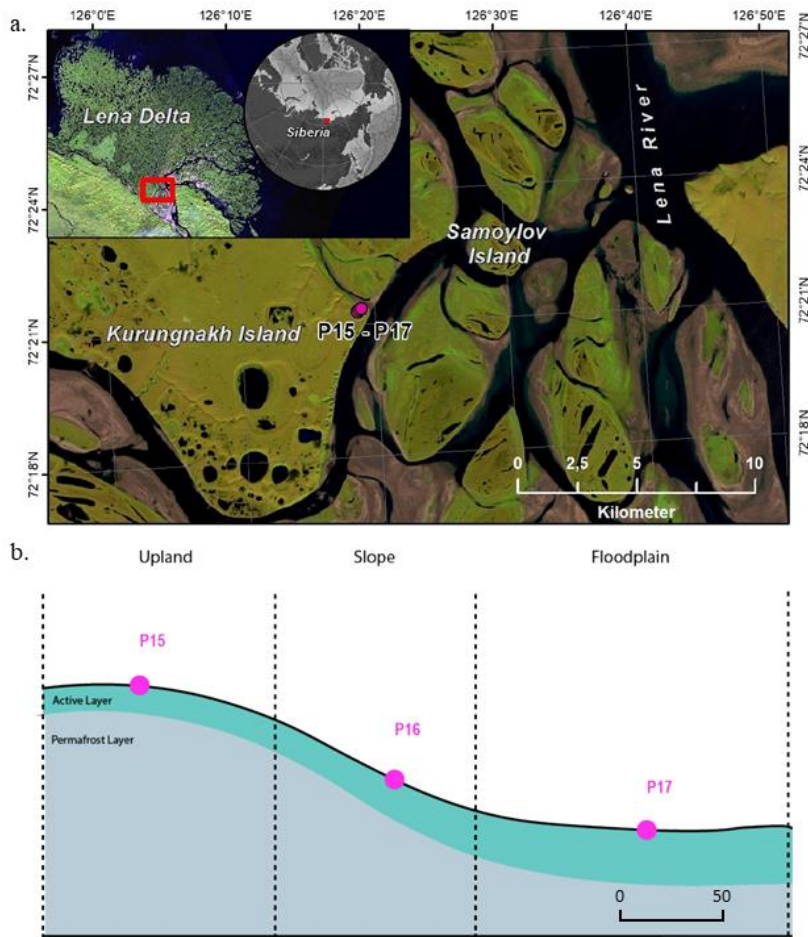


Figure 1: Location of Kurungnakh Island in the Lena Delta (Siberia). The location of the cores used for the study are indicated on the map (a.) and along a schematic transect (b.). Samples were taken during the Lena summer expedition in 2018.

2.2 Sedimentary and geochemical characterization

We characterized the samples for soil texture, C and nitrogen contents, water content, [electronic](#)-conductivity, and pH. First, samples were thawed at 4° C overnight; then the pore water was extracted with a rhizon soil moisture sampler ([Meijboom and van Noordwijk, 1991](#))(Rhizon MOM - 0.6 μm Rhizosphere) ([Meijboom and van Noordwijk, 1991](#)). Electrical conductivity and pH were measured from pore water. Prior to further analyses, soil samples were freeze-dried, and the absolute water content (Eq 1) was calculated. For TOC weight percent, Total Carbon (TC), and Total Nitrogen (TN), subsamples were homogenized and measured with a carbon-nitrogen-sulfur (CNS) analyzer (Elementar Vario EL III). Each subsample was measured in duplicate, and; standards and blanks were used to ensure reliable analytical measurements. The bulk density was determined based on a transfer function between absolute water content and bulk density made by [Fuchs, \(2019\)](#)

135 (Supplementary Fig 2). Since most of the samples used to establish this correlation came from the same area as our samples, we assumed that the transfer function was applicable to our samples.

$$\theta = \frac{W_w - W_d}{W_w} \quad \text{Eq(1)}$$

Where θ is ~~for~~the water content, W_w is wet weight, and W_d dry weight.

140 Carbon ~~storages-were~~storage was calculated by multiplying the TOC contents with the bulk density and then divided by the sample length.

Another subsample was used for grain size characterization. The grain size analysis was conducted using a laser diffraction particle size analyzer (Mastersizer 3000), ~~Company Malvern, Malvern, UK~~. Prior to measuring, subsamples were put on a heated shaker for three weeks, and H₂O₂ was added daily to remove the organic materials. The samples were measured in a wet dispersion unit, and at least three subsamples from each sample were measured. The average grain size distribution (in vol%) was calculated from the measured replicates.

2.3 Incubation set-up and substrate addition

To mimic a wet growing season, the samples were first incubated under anaerobic conditions for 60 days at two different temperatures, 4 °C and 20 °C. Since eleven samples out of twelve did not produce CH₄ after two months incubation, we extended the incubation time to 363 days to see whether the other cores would produce CH₄. For every sample, three replicates were incubated, resulting in a total of 36 samples. Prior to incubation, the samples were thawed at 4°C and prepared under oxygen-free conditions using an anoxic glovebox. The samples were homogenized and ~~13g~~13 g of wet soil was collected and inserted into a 120 mL vial. Sterilized tap water was added only to samples with a gravimetric moisture content of less than 30% to limit the effect of gas dissolution (Henry's Law). The amount of ~~Sterilized~~sterilized tap water was calculated to reach 30% gravimetric moisture, based on the original water content and the weight (wet and dry). The flasks were closed with rubber stoppers and aluminium lids. The headspace of the samples was flushed with pure nitrogen for three minutes to remove potential O₂ inside the vials. ~~The~~Then the samples were incubated in the dark.

After 60 days of incubation, 0.7 mg glucose per gram dry sample weight were added to two of the three replicates to understand the effect of potential substrate limitation in the soil system. The glucose was diluted with milli-Q water to obtain a 100 g.L⁻¹ solution. Solutions were injected via syringe to minimize soil disturbance (Pegoraro et al., 2019)(Pegoraro et al., 2019). The same amount of water as in the glucose solution was added to the third replicate to ensure that differences in gas production were only due to the addition of glucose (Pegoraro et al., 2019; Adamczyk et al., 2021). The glucose addition was also carried out under oxygen-free conditions.

165 The effects of glucose are usually observed within less than ~~48h~~48 h (Yavitt et al., 1997; Pegoraro et al., 2019)(Yavitt et al., 1997; Pegoraro et al., 2019). Therefore, after the glucose addition, gas was measured daily for one week (described in the following section). As the first injection had little effect on gas production, a second injection (day 64) was added with twice the amount of glucose solution (1.4 mg glucose per gram dry sample weight).

2.4 Gas analyses

170 CO₂ and CH₄ in the headspace were measured with a gas chromatograph (GC) (7890A, Agilent Technologies, USA) with flame ionization detection (FID). The temperature in the column was 50 °C with a flow of 15 mL.min⁻¹ and a runtime of 4.5 minutes. Helium was used as a carrier gas. A Hamilton syringe was used to introduce 250 µL of the sampling gas into the GC. For the first week, measurements were made every two days, then twice a week for three weeks, then once a week until day 60. The incubation vials were flushed when either CH₄ or CO₂ concentration reached ~~1x~~10⁴ ppm to avoid gas saturation inside the flask. The production rate was calculated with the change in concentration of CO₂ and CH₄ over the incubation time. First

Field Code Changed

the measured CO₂ and CH₄ concentrations were converted from ppmv to μmol/L using the ~~Ideal Gas Law~~ ideal gas law, then a linear regression between each measurement point was used to calculate the change in concentration over time. The production rate was calculated using the change in concentration over time from the linear regression, then the rates were normalized using the volume of the soil (for differences in the jar headspace) and the weight of the dry soil samples (Robertson et al., 1999). Then these rates were also normalized by the %C found in each sample to look at substrate quality. For samples with pH>7, water contents were very low (Table 1), therefore we assumed that a negligible amount of CO₂ was stored as DIC in the sample water and did not correct the calculation for the pH. However, we are aware that this might underestimate C mineralization.

185 The impact of glucose on CH₄ and CO₂ production was quantified as a glucose factor, calculated using the cumulative C production at 67 days.

$$Gf = \frac{(P_{gt} - P_t)}{P_t}$$

Where Gf is the glucose factor, P_{gt} is total CH₄ production for samples with glucose, and P_t is total CH₄ production.

2.5 Quantification of methanotrophic and methanogenic gene copy numbers

190 Methanogenic archaea were quantified with quantitative Polymerase Chain Reaction (qPCR) at different times during the incubations: when the samples were still frozen (1); after 60 days of incubation (2); and after glucose addition (67 days of incubation) (3). However, due to laboratory restrictions during the Covid-19 pandemic, it ~~has~~ was not ~~been~~ possible to analyse all the incubated vials. Only one replicate per sample for the first two runs were analysed. For the last run, we selected the two samples with the highest CH₄ production rates after the glucose addition – the active layers of P16 and P17.

195 Since ~~methanotroph~~ methanotrophic bacteria are good indicators of the oxidation level under in-situ ~~condition~~ conditions, they were quantified with qPCR before starting the incubation.

Key genes ~~coding for~~ encoding the enzyme methyl coenzyme-M reductase (*mcrA*) (~~Thauer, 1998~~)(Thauer, 1998) and for the enzyme particulate methane monooxygenase (*pmoA*) (~~Theisen and Murrell, 2005~~)(Theisen and Murrell, 2005) were examined to identify methanogens and methanotrophs, respectively. DNA extractions were performed with a GeneMATRIX Soil DNA purification kit (Roboklon, Germany) according to the manufacturer's protocol. After DNA extraction, the DNA concentration was quantified by fluorescence with the Qubit dsDNA HS Assay Kit (Invitrogen/Invitrogen, United States). Gene copy numbers were quantified using a SYBRGreen qPCR assay using the KAPA SYBRFAST qPCR Master Mix (Sigma-Aldrich, Germany) on a CFX96 real-time thermal cycler (Bio-Rad Laboratories Inc., United States). All runs were performed in technical triplicates, and each run was completed through melt-curve analysis in order to check for specificity of the assay (~~Liebner et al., 2015~~)(Liebner et al., 2015). Methanogenic archaea were targeted with the primer set mlas-F/*mcrA*-R (~~Hales et al., 1996~~)(Microsynth, Balgach, Switzerland) (Hales et al., 1996).

To amplify the methanogenic archaea *mcrA* gene, PCR samples were kept at 95 °C for 5 min to denature the DNA. The amplification process was performed with 40 denaturation cycles at 95°C for 1 min, annealing at 60 °C for 45 s, and elongating at 72 °C for 90 s. To ensure complete amplification, samples were kept at 80 °C for 10 min. In addition, to amplify the methanotrophic *pmoA* gene, using primer pmoA189-F and primer pmoAmb661-R two PCR reaction conditions were used. The first PCR comprised initial denaturation at 95 °C for 5 min, 30 cycles with denaturation at 94 °C for 45 s, decreasing annealing temperature from 64 °C to 52 °C for 60 s, elongation at 72 °C for 90s, and final elongation at 80 °C for 90 s. The second PCR comprised an initial denaturation and polymerase activation at 95 °C for 5 min, 22 cycles of denaturation at 94 °C for 45 s, annealing at 56°C for 60 s, elongation at 72 °C for 90 s, and a final extension at 72 °C for 10 min.

215 2.6 Statistical analyses

The gas production and microbial data did not show a normal distribution; consequently, it was not possible to test for differences by performing an ANOVA. The differences between cores and depths, and also the impact of temperature on gas production and microbes, were therefore tested using the Kruskal-Wallis test with the R function, `kruskal.test()`.

220 [All statistics and results analyses were performed with R version 4.0.5 \(R Core Team, 2021\)](#)[All statistics and results analyses were performed with R version 4.0.5 \(R Core Team, 2021\).](#)

3 Results

3.1 Soil characteristics

225 All soil samples had a pH between 6.5 -7.5, except P15-F. Most electrical conductivities were very low ($<200 \mu\text{S}\cdot\text{cm}^{-1}$), except for two samples: P16-F and P17-A (Table 2). Water content was higher in permafrost (54.5%-60.8%) than in the active layer (23.7%-25.8%) for the two yedoma cores, P15 and P16. The water content was higher in the active layer than the permafrost layer in the floodplain core P17 (36.2% vs. 17.2%; Table 2).

Sediment TOC ranged from 0.2% to 3.8%. Most TOC contents ranged from 2.7% to 3.8% but the TOC content in the permafrost layer of P17 was the lowest of the six samples (0.17%; Table 2). All the samples had TOC below 6%, and therefore they were considered as mineral soils ($\%C < 12\%$) (Table 2) ([Soil Survey Staff, 2014](#))([Soil Survey Staff, 2014](#)). TN contents 230 were very low for all the samples ($<0.3\%$) and was below the detection limit of the laser analyzer (below 0.1%) for P17-F. C:N ratios ranged between 12 and 20. The highest ratios were measured in P15; the lowest were in P16. The C:N ratio was higher in the permafrost layer of P15 than in the active layer.

The C stock ranged from 2.3 to 38.8 $\text{kg}\cdot\text{m}^{-3}$. The active layers for all the samples were higher than 30 $\text{kg}\cdot\text{m}^{-2}$ while, the highest C stock in the permafrost layer was 19 $\text{kg}\cdot\text{m}^{-3}$ in the Yedoma core P16. The permafrost layer of the floodplain had the lowest 235 C storage, more than ten times lower than samples from the active layers (Table 2).

The grain size distribution was similar between P15 and P16. The active layer of P17 contained more clay and the least sand of the other samples, while permafrost in P17-F was the sandiest sample (Supplementary Table 1).

Table 1: Soil description and vertical position of the sampling cores.

<i>Samples</i>	<i>Depth (cm)</i>	<i>Layer</i>	<i>Horizon</i>	<i>Soil description</i>
<i>P15-A</i>	41.5	Active	Mineral	Compacts silt, grey, with brown organic inclusions
<i>P15-F</i>	81.5	Permafrost	Mineral	Ataxilic ice structure, silt grey
<i>P16-A</i>	38.5	Active	Mineral	Silt, brown, organic rich, slightly sandy
<i>P16-F</i>	102.5	Permafrost	Mineral	Silt, grey-brown, structureless to micro-lenticular
<i>P17-A</i>	31.5	Active	Mineral	Organic rich silt, slightly sandy
<i>P17-F</i>	78.5	Permafrost	Mineral	Sand, no visible ice

Table 2: Chemical and physical properties of the active and frozen layers of the three cores. The conductivity temperature reference was 25°C. Numbers in brackets are standard deviations

<i>Samples</i>	<i>pH</i>	<i>Conductivity</i> ($\mu\text{S/cm}$)	<i>TOC (%)</i>	<i>C/N ratio</i>	<i>TN (%)</i>	<i>C (kg.m⁻³)</i>	<i>Water content (weight %)</i>
<i>P15-A</i>	6.75	164.5	3.54	18.13	0.1975	38.8	25.8
<i>P15-F</i>	6.06	150.2	2.70	20.59	0.133	9.4	60.8
<i>P16-A</i>	7.21	98.6	2.70	12.95	0.211	35.2	23.7
<i>P16-F</i>	7.06	479	3.81	12.67	0.3085	18.5	54.5
<i>P17-A</i>	7.22	635	3.48	18.46	0.1935	30.0	36.2
<i>P17-F</i>	7.44	86.4	0.17		< 0.10	2.3	17.2

3.2 Potential gas production

3.2.1 CH₄ production over one year of incubation

At the end of 363-day incubation, four of the six samples produced CH₄ at 20 °C incubation temperature (Figure 2; Figure 3). The floodplain active layer (P17-A) was the sample with the highest cumulative CH₄ production over the incubation time (917.2 ± 150 μg CH₄-C g⁻¹ DW⁻¹). After 6 months of incubation, the CH₄ production rate of P17-A decreased and then plateaued. The floodplain permafrost core (P17-F) produced 1% of ~~this~~ the amount of CH₄ produced by the active layer from the same core (0.5 ± 0.2 μg CH₄-C g⁻¹ DW⁻¹) at 20 °C. The permafrost layers at 20 °C of both Yedoma cores (P15 and P16) produced similar amounts of CH₄ (20.5 ± 6.1 μg CH₄-C g⁻¹ DW⁻¹ DW and 159 ± 104 μg CH₄-C g⁻¹ DW⁻¹, respectively) while CH₄ production from the active layers of these cores was minimal (P16-A: 3.34 ± 0.25 μg CH₄-C g⁻¹ DW⁻¹; P15-A: 0.51 ± 0.14 μg CH₄-C g⁻¹ DW⁻¹ DW). Cumulative CH₄ production at 4 °C was limited to one sample, the active layer of the floodplain core (Figure 2; Figure 3). Cumulative production of the other cores was less than 1 μg CH₄-C g DW⁻¹ after 1 year (Figure 2a; Figure 2b; Figure 3).

The lag time before CH₄ production was observed ranged from 14 days to over 363 days. The active layer of the floodplain core (P17-A-20) was the first to produce CH₄ after 14 days of incubation at 20 °C. The frozen layers of Yedoma the cores required at least 6 months incubation to start producing CH₄ at 20 °C (Figure 2; Table 2), but in the active layer of the Yedoma cores, CH₄ production took substantially longer: 273 days for P16-A-20, while P15-A did not produce appreciable CH₄ over 363 days in the experiment. At 4 °C, CH₄ production in P17-A started after 333 days but was not observed for the other samples (Figure 2; Table 3).

3.2.2 CO₂ production over one year of incubation

Over the 363-day incubation, cumulative CO₂ production ranged from 90.3 μg CO₂-C g⁻¹ DW to 701.4 μg CO₂-C g⁻¹ DW. The cumulative CO₂ production of P17-A at 20 °C was the highest among all the samples (701.4 ± 124 μg CO₂-C g⁻¹ DW⁻¹ DW), while the permafrost layer of the same core at 20 °C was the lowest (Figure 2; Figure 3). The CO₂ production of P15 and P16 were in the same range, between 142 ± 85 μg CO₂-C g⁻¹ DW (P16-A at 4 °C) and 348.3 ± 135 μg CO₂-C g⁻¹ DW⁻¹ DW (P15-F at 20 °C) (except P16-F at 4 °C); (F-Kruskal-WallisChi squared = 2.80, df = 1, p = 0.20) (Figure 2; Figure 3). At 4 °C, the permafrost layers of the Yedoma core P16 and the floodplain core P17 had cumulative production below 60 μg CO₂-C g⁻¹ DW⁻¹ DW. The results per g C g C showed a different pattern for the cumulative CO₂ production of the floodplain core P17. The permafrost layer at 4 °C reached 7.98 mg CO₂-C g C g⁻¹ C and had higher CO₂ production than the permafrost layer at 20 °C and the active layer at 4 °C. (Supplementary Fig 3)

A decrease of CO₂ production at the beginning of the incubation was observed for all the samples (Figure 2, Supplementary Fig 4). All the active layer samples (except the active layer of the floodplain P17 at 4 °C), as well as the permafrost layers of the Yedoma cores P15, and P16 at 20 °C, reached the maximum production rates of CO₂ before or at the end of the first two months (Figure 2). The maximum production rate of CO₂ for the active layer of the floodplain at 4 °C was attained after 300-day incubation, and the other permafrost samples reached the maximum production rate between two and five months (Figure 2). Maximum production rates ranged between 57.13 μg C-CO₂ g C⁻¹ d⁻¹ (P16-A) and 754 μg C-CO₂ g C⁻¹ d⁻¹ (P17-F) at 4 °C, and between 120.54 and 510.65 μg C-CO₂ g C⁻¹ d⁻¹ for P16-F and P15-A, respectively, at 20 °C (Supplementary Table 2). After half a year of incubation, CO₂ production plateaued for all the samples, except for the active layer of the floodplain sample at 4 °C. For all the samples, we noticed an increase in CO₂ production after 60-day days of incubation, e.g., after the microbial sampling, following followed by a decrease in the CO₂ production. We did not consider those results to describe the maximum production rates.

After one year of incubation, neither the temperature nor the depth impacted the cumulative CO₂ production of the cores ($F=$
 $Kruskal-WallisChi\ squared = 3.86$, $df = 1$, $p = 0.09$), Figure 2, Figure 3). CO₂ production was higher at 20 °C only for the
 285 permafrost layer of the Yedoma core P16 and the active layer of the floodplain P17 ($F=Kruskal-WallisChi\ squared = 3.86$, df
 $= 1$, $p < 0.05$) (Figure 2; Figure 3).

The P17-A-20 CO₂:CH₄ ratio decreased rapidly during the first 14 days. The CO₂:CH₄ ratio reached one after 40 days and
 remained stable until the end of incubation (

Table 3). As well, the CO₂:CH₄ ratio of P17-A at 4°C and P16-F at 20 °C were low after 363 days of incubation (respectively,
 2.7 ± 2.7 and 2.5 ± 2.1). For all the samples, except P15-F, CO₂:CH₄ ratios were significantly lower at 20 °C than at 4 °C ($F=$
 290 $Kruskal-WallisChi\ squared = 3.92$, $df = 1$, $p < 0.05$) (Table 3).

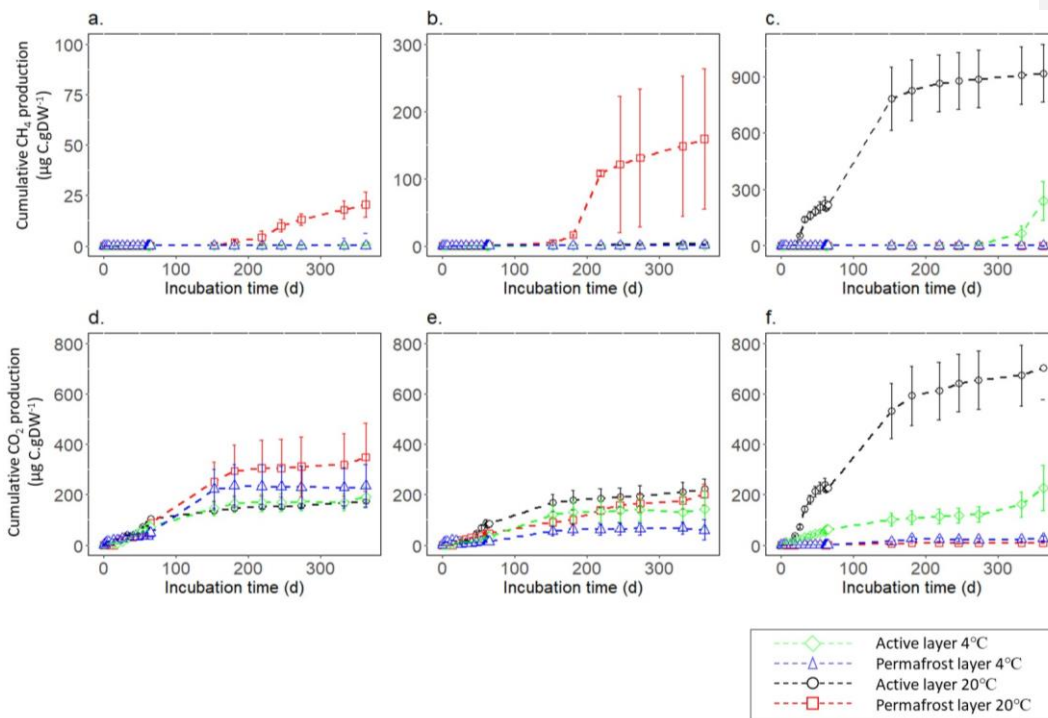


Figure 2: Cumulative gas production per gram dry weight (DW) at 4 °C and 20 °C for 363 days of incubation. CH₄ production of (a.) P15, (b.) P16 and
 (c.) P17. CO₂ production of (d.) P15, (e.) P16 and (f.) P17. Error bars show the standard deviation from the means ± standard error (n=3). Note differing
 y-axis scales between cores for CH₄

295

Figure 3: Cumulative production of CO₂ and CH₄ per gram dry wet of CO₂ and CH₄ after 60 days of incubation at 4°C and 20°C and after 363 days. AL stands for “Active layer” and PL stands for “Permafrost Layer”. Scale is expressed as square root in order to have for a better display representation of the data.

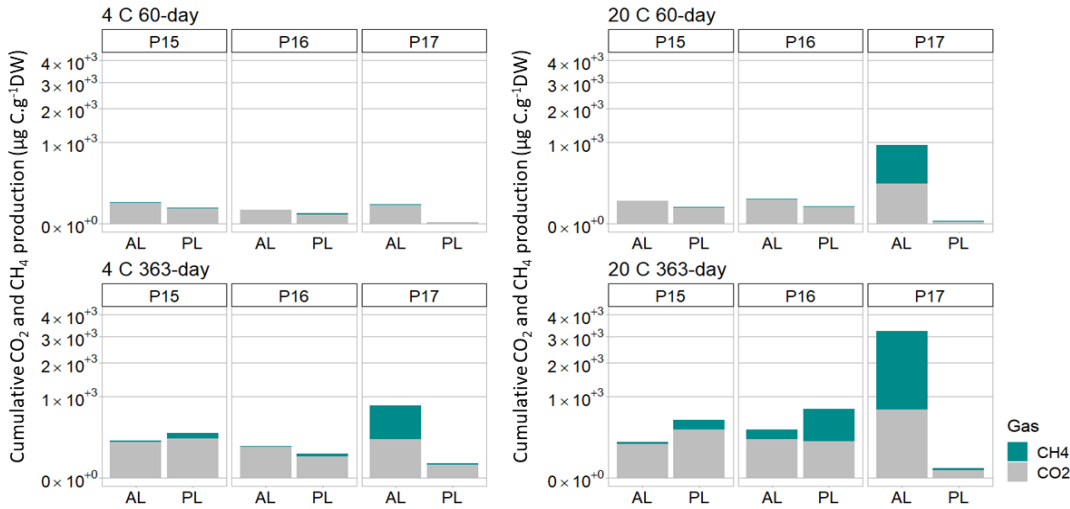


Table 3: Summary table of lag time of CH₄ offset, CO₂:CH₄ ratios, and glucose factors. Lag time is expressed in days, L.T. stands for samples where the lag time did not end after 1 year incubation. CO₂:CH₄ ratios represent means of total production after 363 days of incubation at 20 °C and 4 °C after 363 days of incubation. Glucose factors were calculated based on cumulative C production 7 days after glucose addition for each sample with total C productions. Positive values indicate positive impact of glucose on GHG production and while negative values means indicate less GHG production after glucose addition.

Samples	Layer	Lag Time (days)		Mean CO ₂ :CH ₄		Glucose Factor			
		20 °C	4 °C	4 °C	20 °C	CH ₄ 4 °C	CH ₄ 20 °C	CO ₂ 4 °C	CO ₂ 20 °C
P15-A	Active	L.T.	L.T.	522.6 ± 1.7x10 ⁻²	409.1 ± 2.2x10 ⁻²	-0.10	-0.38	0.02	0.18
P15-F	Permafrost	153	L.T.	1930.1 ± 2.2x10 ⁻³	2236.8 ± 3.9x10 ⁻³	0.02	-0.31	-0.20	-0.44
P16-A	Active	274	L.T.	1661.4 ± 1.5x10 ⁻²	50.1 ± 4.0x10 ⁻¹	-0.41	0.70	-0.02	1.22
P16-F	Permafrost	181	L.T.	195.5 ± 1.3x10 ⁻²	2.5 ± 2.1	0.40	-0.93	0.11	3.23
P17-A	Active	14	333	2.7 ± 2.7	0.8 ± 0.1	-0.01	0.24	0.51	0.60
P17-F	Permafrost	L.T.	L.T.	266.9 ± 1.8x10 ⁻²	34.8 ± 4.2x10 ⁻¹	1.18	0.27	-0.11	0.82

3.2.3 Effect of glucose addition

Overall, no effect of glucose injection on CH₄ production was detected after 67-day incubation (

315 Table 3) (~~F=Kruskal-WallisChi squared = 0.25~~, df = 1, p = 0.5913). A ~~CH₄~~ production peak was detected one day after the second glucose addition for P15 and P16. The response factors were low (CH₄ production between 1.2 and 1.7 times higher with glucose addition ~~than without~~) and appeared only at 20 °C. No impact ~~fromof~~ the glucose addition was detected on CH₄ production for the samples at 4 °C, ~~neither~~ after ~~either~~ the first ~~enor~~ the second injection (Supplementary ~~FigFigure~~ 5).

320 CO₂ production at 20 °C was in overall increased by glucose (~~F=Kruskal-WallisChi squared = 3.78~~, df = 1, p < 0.05). The maximum increase of CO₂ production was seen for the permafrost layer of P16 (4.2 times higher with glucose addition). No difference in CO₂ production was detected for any of the samples at 4 °C after glucose addition (Supplementary Figure 5).

3.3 Gene copy numbers of methanogens and methanotrophs

For half of the samples, no methanogenic gene copy numbers were detected when the samples were thawed prior to beginning the incubation. From these samples, only the methanogenic gene copy number for core P17-A ~~were~~ above the detection limit (4.3x10³). Therefore, it was not possible to compare the methanogenic gene copy numbers before the ~~beginningstart~~ of the incubation (Figure 4).

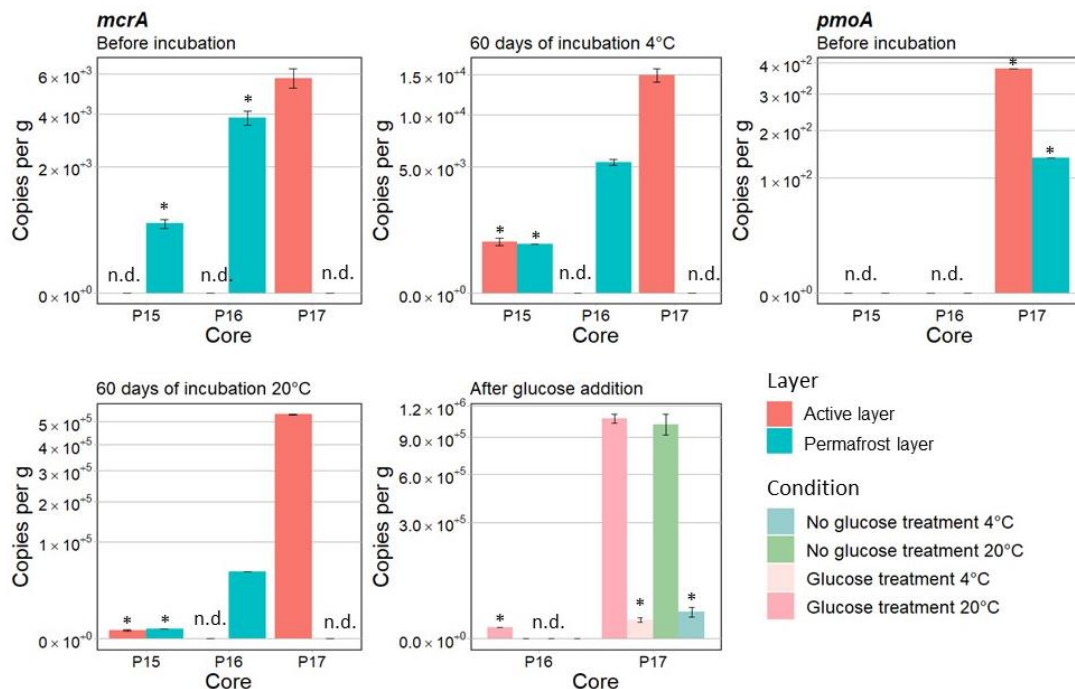
325 After 60 days of incubation, the *mcrA* gene copy numbers ranged from 5.35x10³ to 5.34x10⁵. The qPCR results showed significant differences between cores after 60 days of incubation (~~F=Kruskal-WallisChi squared = 3.89~~, df = 1, p < 0.05) with the highest copy number per gram soil (Figure 4c) in P17-A. No methanogenic gene copy numbers were detected for the permafrost layer of P17, as well as the active layer of P16.

330 P16-F and P17-A had 9 ~~times~~ and 36 times higher ~~copies~~*mcrA* copy number per gram soil, respectively, at 20 °C than at 4 °C (~~F=Kruskal-WallisChi squared = 3.9~~, df = 1, p < 0.05) (Figure 4). The temperature response for the active and permafrost layer of P15 was not identified because the results were below ~~the~~ detection limit ~~at both~~ at 4 °C and 20 °C.

Similarly, no comparison was possible between active and permafrost layers for all the samples.

335 Gene copy numbers of methanotrophic bacteria based on the *pmoA* gene, ~~before the incubation~~, were either below detection limit, or not detected ~~before the incubation~~, therefore no interpretation on the oxic conditions under field condition was possible (Figure 4).

~~Gene copy~~Copy numbers after addition of glucose did not differ from those without glucose (Figure 4).



340 Figure 4: Means of gene copies per gram calculated with qPCR amplification at different times, time for different conditions - before
 345 the incubation, after 60 days of incubation, and at the end. Gene copy numbers of *mcrA* were calculated for P15, P16, and P17. *mcrA*
 results are shown for the active layers of P16 and P17 with or without glucose treatment after 67 days of incubation. Gene copy
 numbers of *pmoA* are shown for P15, P16, and P17 before the incubation. Samples below detection limit are indicated by * and
 samples where copies per gram were not detected are indicated by n.d. Scale is expressed as square root in order to have a better
 display.

4. Discussion

4.1. CH₄ production in floodplain environment and Yedoma cores across landscape positions

4.1.1. Floodplain core

We mimicked potential CH₄ production during a growing season (60 days) in a floodplain environment of Kurungnakh Island
 350 in the Lena River Delta, and extended the incubation time to one year to capture the CH₄ production behavior. Within the first
 two months, the results showed high rates and quick onset of CH₄ production as well as presence of methanogen communities
 (Figure 4) in the active layer of the floodplain core P17 at 20 °C only. Those findings, as well as the low CO₂:CH₄ ratio,
 indicated a quick establishment of optimum methanogenic conditions within the growing season time frame of 60 days
 (Symons and Buswell, 1993) (Figure 2c, Figure 3, Table 3Table 2). Herbst, (2022) did a similar incubation study with samples
 355 from the active floodplains of Kurungnakh Island and nearby Samoylov Island (Figure 1). CH₄ was produced from two of the
 three cores within the first 60 days of incubation (Supplementary Table 3). In both this study and the Herbst study, CH₄
 production was triggered quickly after the beginning of incubation (from 10 to 40 days) from these floodplain samples. Thus,
 these Arctic floodplain environments may allow the fast establishment of methanogens, and therefore, rapid CH₄ production
 under anaerobic conditions.

360 However, not all floodplain soils showed fast establishment of methane communities and high rates of potential methane production. Unlike the active layer, the permafrost layers of floodplain did not produce appreciable CH₄ after one year incubation at either 4 °C or 20 °C and were still considered in the lag phase. The absence of detectable *mcrA* copy numbers per gram soil after 60 ~~day days of~~ incubation indicated the absence of methanogen communities in the permafrost samples (Figure 4). Similarly, low rates of CO₂ production, low C content, and high sand content in this permafrost sample indicate ~~difficult non~~
365 ~~suitable~~ conditions for many types of soil microbes (Figure 2, Figure 4, Table 1) ~~)-~~ (Eskelinen et al., 2009). As expected, our results showed significant differences between CH₄ production rates at 4 °C and 20 °C. At 4 °C, almost 300-days of incubation were needed to trigger CH₄ production in the active layer of the floodplain (versus 14 days at 20 °C), with a total cumulative CH₄ production four times lower than at 20 °C (Figure 3). Other studies showed similar patterns, e.g., CH₄ production increases with temperature and has shorter lag times (Ganzert et al., 2007; Treat et al., 2015). This is explained by
370 a strong temperature sensitivity of methanogen communities (Westermann, 1993; Li et al., 2015). At the end of the growing season simulation, our results showed ~~the~~ *mcrA* copy numbers 36 times lower at 4 °C than at 20 °C (Figure 4), again indicating that the methanogen community required both time and ~~warm~~ high temperatures to establish.

4.1.2. Yedoma cores

This study highlights a different CH₄ production behavior between the floodplain and the Yedoma cores. The permafrost layers
375 from the Yedoma cores only started producing CH₄ after six months of incubation at 20 °C, whereas the floodplain core produced CH₄ earlier (Figure 2). The CO₂:CH₄ ratios remained high after one year of incubation (Table 3), meaning that the methanogenic conditions were not yet optimum (Symons and Buswell, 1993). The low ~~mCRAmcrA~~ copies after the 60 ~~day days of~~ incubation compared to the active layer of the floodplain, as well as the long lag times, showed that the methanogen communities took more time to ~~activate become active~~ in the permafrost Yedoma cores (Figure 2, Figure 4).
380 Our results indicated higher CH₄ production rates in the permafrost layer than in the active layer, while others generally show the opposite (Yavitt et al., 2006; Treat et al., 2015, p.201). However, most of the studies on CH₄ production from Yedoma cores showed high variability in the cumulative CH₄ production. As explained above, lag times measured from former studies differed as well as CH₄ production rates (Lee et al., 2012; Knoblauch et al., 2013; Walz et al., 2018; Jongejans et al., 2021). It is therefore ~~hard~~ difficult to estimate the potential production of CH₄ after thaw from Yedoma soils after thawing due to this
385 high variability. Methanogens are highly constrained microbial communities, and the community size varied strongly between the sites in this study (Figure 4), which partly explains the discrepancies among the studies on Yedoma soils due to the ecological and phylogenetic narrowness of the methanogen communities (Ernakovich et al., 2022).
The active layers at 4 °C and 20 °C and permafrost layers at ~~the lower temperatures~~ 4 °C were still in the lag phase without appreciable CH₄ production after ~~the~~ one year of incubation (Figure 2, Figure 3, Table 3), which agrees with the absence of
390 detected methanogen community (Figure 4). Several multiannual studies observed also long and heterogeneous lag times at 4 °C for Yedoma soils (from 53±23 to up to 2500 days; Knoblauch et al., 2018; Walz et al., 2018). Knoblauch et al., (2018) explained the long lag time by a lack of methanogens, or a lack of active methanogenic communities in soil samples. We added glucose to test whether the absence of CH₄ production was due to a lack of labile C or to a lack of established methanogenic communities. If the methanogen community was small, but established, we would expect to have community growth after the
395 glucose addition. Since, glucose had no effect neither on CH₄ production rates nor on P15 and P16 methanogen community growth, we concluded that the absence of CH₄ production for those samples was because the methanogens were not active (or not active enough to detect). It has been shown that the establishment of microbial community after thaw is correlated to the community characteristics as well as the thaw disturbance (Deng et al., 2015; Ernakovich et al., 2022). For ecologically and phylogenetically narrow microbial communities, like methanogens, random environmental processes like microtopography
400 (stochastic processes) strongly influence the abundances and activation of the microbial communities. After an abrupt thaw, like we simulated in our incubation study, the role played by stochastic processes on constrained microbial communities is

even stronger (Deng et al., 2015; Ernakovich et al., 2022). Therefore, although ~~we the incubation was~~ carried out ~~incubation~~ under anaerobic conditions, the quantity and the establishment of active methanogen community ~~in the~~ samples after thaw was strongly ~~controlled by stochastic processes~~.

Commented [ML1]: What does that mean, specify.

405 4.1.3. Controls on CH₄ production across landscape positions

CH₄ production over the incubation time was not correlated with the TOC and TN% (Figure 3, Table 2). The landscape position rather than soil characteristics played a key role in the establishment of ~~microbe activities~~ ~~microbial activity~~ and, consequently, explained much of the variation in GHG production among the samples. Periodic water saturation in core P17 was indicated by oxidation marks at several depths in the field. These redox features indicate periodically anoxic conditions that likely favoured the establishment or persistence of methanogen communities and reduced the lag times prior to CH₄ production under anaerobic conditions (Chasar et al., 2000; Paul et al., 2006; Jaatinen et al., 2007; Keller and Bridgham, 2007; Figure 2, Table 3). On the other hand, well-drained conditions were found in the field for the active layers of both the upland and the slope cores (P15 and P16), which did not produce appreciable CH₄ after one ~~year of~~ incubation (Figure 2, Figure 3). The aerobic conditions due to the dry environment likely inhibited methanogenesis (Meronigal and Schlesinger, 2002). Unlike the active layers, the permafrost layers of Yedoma showed low but existing *mcrA* results from the Yedoma permafrost layers at 20 °C (Figure 4), and started producing CH₄ after six months. The methanogen community was likely established prior ~~to~~ or during the deposit of the Yedoma sediments and the microbial community survived although it was freeze-locked (Holm et al 2020). ~~Additionally~~ ~~In addition~~, we quantified methanotroph communities to include more information about the potential for methane oxidation under field conditions, but the results showed amounts below detection ~~limit~~ before the incubation (Figure 4). These results support our hypothesis concerning the impact of landscape position on CH₄ production: aerobic conditions in the landscape coincided with poor establishment of methanogenesis even when incubation conditions become favourable for methanogens.

4.2. Controls on potential CO₂ production

~~Our~~ ~~The~~ rates of CO₂ production per g C were in the same order of magnitude as other Yedoma incubation studies from Kurungnakh Island (Knoblauch et al., 2013, 2018) and nearby Lena ~~River~~ ~~Delta~~ ~~River~~ (Walz et al., 2018). These similar results suggest that C in these Yedoma soils is easily available due to the organic-rich characteristics (Strauss et al., 2013). On the other hand, the adjacent samples from the permafrost layers of the floodplain showed CO₂ production g per ~~C~~ ~~gram~~ similar to the Yedoma cores, while, it had the lowest CO₂ cumulative production per gram dry weight of soil. Although floodplain environments in the Lena Delta are considered as a low C ~~content~~ pool (Siewert et al., 2016), our results showed that the C in ~~the soils~~ ~~this soil~~ was highly labile and comparable to the lability of Yedoma soils.

The CO₂ production followed trends in total C and N contents. The samples with similar C and N contents produced comparable ranges of CO₂, whereas the sample (P17-F) with the lowest TOC and N content showed low CO₂ production (~~per~~ ~~gram~~ ~~per~~ ~~DW~~) during ~~the~~ incubation (Figure 2, Table 2, Supplementary Table 2). As shown by Schaedel et al. (2014), the C:N ratio was positively correlated to the cumulative CO₂ production. However, the correlation was stronger at 4°C than 20 °C (Supplementary Fig 7). Therefore, consistent with other studies (Schädel et al., 2014; Knoblauch et al., 2018), the quality (N), quantity (C), and the bioavailability (C:N) of the OM is a key factor for the mineralization into CO₂ production.

Our CO₂ and CH₄ production results combined with microbial analysis indicated that CO₂ production pathways might change according to the landscape position. The ~~4:1~~ ~~CO₂:CH₄~~ production ratio ~~of 1:1~~, as well as the presence of ~~a~~ high number of methanogenic archaea, indicated that the CO₂ production in the active layer floodplain could have ~~come~~ ~~originated~~ from methanogenesis (Figure 3, Figure 4) (Symons and Buswell, 1993; Knoblauch et al., 2018; Holm et al., 2020). In drier environments, like the P15 and P16 cores, the high CO₂:CH₄ production rates resulted from other, undetermined anaerobic

decomposition pathways. Anaerobic respiration is a common function, and diverse microbial communities are able to decompose the OM to CO₂, therefore, the anaerobic microbial community is not a limiting factor for C mineralization into CO₂ (Elderfield and Schlesinger, 1998). Based on the positive correlation between C:N and the cumulative CO₂ (Supplementary Fig 7), and the broad microbial community able to produce CO₂, our CO₂ production is rather controlled by the quality (N) and the quantity (TOC) of the OM than the microbial communities (Knoblauch et al., 2018; Holm et al., 2020).

4.3. Implication for C feedback in Kurungnakh Island during the growing season

With climate change, Arctic environments will be subject to changes in moisture conditions, vegetation shifts, increased active layer depth and abrupt permafrost thaw (Serreze et al., 2000; Hinzman et al., 2005; Myers-Smith et al., 2011; Turetsky et al., 2019). Our permafrost thaw simulation under wet summer conditions for Kurungnakh Island soil showed that the CO₂ production for the Yedoma cores was similar in magnitude to other studies including Yedoma. Under soil. In the incubation experiment, all the Yedoma samples reached the maximum production rates within the first two months of incubation (Figure 2). Schädel et al. (2014) attributed the decrease in CO₂ production rates after some time in incubations to a rapid C turnover that relied mainly on the decomposition of the labile C pool (Schädel et al., 2014; Walz et al., 2018; Schädel et al., 2020). However, several studies pointed out the small size of the labile C pool of Yedoma deposits (Knoblauch et al., 2013; Strauss et al., 2013b). Here, the Yedoma soils from Kurungnakh Island, showed labile C pool depletion after six months of incubation (e.g., the CO₂ production rates decreased and the cumulative CO₂ production plateaued after six months of incubation; Figure 2). Therefore, under wet summer conditions, it is likely that there will be rapid C turnover and CO₂ production during the growing season.

The active layer of the floodplain at 20 °C produced up to 300 µg CH₄-C g⁻¹ DW⁻¹ DW at the end of the simulated growing season. The low-lying position of the floodplain allows regular flooding from the river. The hydrological conditions of this area provide favorable redox conditions, i.e., anaerobic conditions, for the establishment of active methanogen communities if the temperature is high enough (Figures 3, 4). Therefore, we expect CH₄ production from the floodplain site relatively quickly after the beginning of the growing season. Long-term *in situ* measurements in the Lena Delta have shown the highest CH₄ emission rates for moist to dry dwarf shrub-dominated tundra, located mainly in lower floodplain environments (5048.5 mg m⁻² yr⁻¹; Schneider et al., 2009). In this area of the Lena Delta, CH₄ emissions have been measured from June to September, with the highest emission rates in July (Rößger et al., 2022). Our results showed a high CH₄ production potential from the floodplain, however, floodplain environments are periodically flooded, meaning there might be periods where the floodplain would be too dry to allow CH₄ production (Huissteden et al., 2005; Oblogov et al., 2020). A long-term study like by Rößger et al. (2022) in floodplains environments would help to quantify CH₄ emissions from floodplains, how often it occurs during the growing season, and how the CH₄ flux would respond to changes in soil moisture over time.

While CH₄ production did occur in the year-long anaerobic incubation of Yedoma samples, other factors might result in these tundra regions still remaining a net CH₄ sink barring abrupt permafrost thaw (Schneider et al., 2009; Juncher Jørgensen et al., 2015). In these dry Yedoma sites, the net CH₄ flux is the balance between CH₄ production in anoxic soil layers and CH₄ oxidation in overlying aerobic layers. Here, we showed that CH₄ production was possible from these soils given high enough temperatures (Figure 3), but required a long lag time for the establishment of the methanogen communities (Figure 4). Therefore, it is unlikely that the active methanogen communities have enough time (>60 days; Figure 4) or warm enough temperatures (Figure 3) to establish during the growing season in the upland and the slope areas (P15, P16) on Kurungnakh Island even with deeper active layers, soil moisture increases, and highly bioavailable C in Yedoma sediments (Anthony et al., 2014; Mann et al., 2014; Spencer et al., 2015). These conditions may constrain the potential CH₄ emissions from some Yedoma soils even with warmer climates, wetter soils, and permafrost thaw, but will require additional field-based observations to account for plant transport and methane oxidation processes occurring in-situ.

485 5 Conclusion

In this study we provide new information regarding the importance of the landscape position ~~infor~~ CH₄ production during the growing season in Kurungnakh Island ~~in the Lena River Delta~~. High CH₄ production was measured in waterlogged (floodplain) areas within the 60 days simulation of the growing season at 20 °C, thanks to a fast establishment of the methanogen community (14 days). In contrast, the well-drained Yedoma active layer samples were still in the lag phase at the end of the growing season simulation and did not produce appreciable CH₄ emissions, and C turnover ~~came from~~ ~~resulted in~~ CO₂ production. CH₄ was produced by the Yedoma permafrost layers after a lag phase of six months at 20 °C. Although the permafrost layer of the floodplain had low TOC, we identified similar C lability for the three cores as for other studies with samples from Siberia, and therefore high potential C ~~gas~~ production throughout this region, but mainly as CO₂. As a result, the data presented in this case study contribute to ~~quantify~~ ~~quantifying~~ and ~~understand~~ ~~understanding~~ C turnover in permafrost areas. Questions remain regarding how to upscale results from laboratory incubation to in-situ conditions, and our results highlighted the need to better understand changes in redox conditions across the landscape position to improve upscaling.

Author contributions

M.L., C.T. and S.L. designed the study. M.L. conducted all the experiments (soil analyses, incubations, and microbe quantification). M.F. and A.R. collected the soil samples and field notes during the expedition in 2018 and created the map. S.L. furnished laboratory materials to perform microbe analyses and gas measurements. T.H. provided data from her incubation experiments. M.L. wrote the manuscript with contributions from all the co-authors.

Acknowledgments

Funding for this study was provided by ERC-H2020 #851181 FluxWIN, the Helmholtz Impulse Initiative and Networking Fund. Samples were collected during the joint Russian-German LENA 2018 expedition to Samoylov Island within the framework of the BMBF KoPf (Kohlenstoff in Permafrost) project (#3F0764B). This project was also supported by the European Erasmus+ programme. We thank the staff at the Samoylov Research Station for support and logistics during the fieldwork. We also thank the Alfred-Wegener Institute and GFZ lab technicians in Potsdam for laboratory assistance.

References

Adamczyk, M., Rütthi, J., and Frey, B.: Root exudates increase soil respiration and alter microbial community structure in alpine permafrost and active layer soils, *Environmental Microbiology*, 23, 2152–2168, <https://doi.org/10.1111/1462-2920.15383>, 2021.

AMAP: Arctic Climate Change Update 2021: Key Trends and Impacts. Summary for Policy-makers, 2021.

Andreev, A. A., Grosse, G., Schirrmeister, L., Kuznetsova, T. V., Kuzmina, S. A., Bobrov, A. A., Tarasov, P. E., Novenko, E. Y., Meyer, H., Derevyagin, A. Y., Kienast, F., Bryantseva, A., and Kunitsky, V. V.: Weichselian and Holocene palaeoenvironmental history of the Bol'shoy Lyakhovsky Island, New Siberian Archipelago, Arctic Siberia, *Boreas*, 38, 72–110, <https://doi.org/10.1111/j.1502-3885.2008.00039.x>, 2009.

Anthony, K. M. W., Zimov, S. A., Grosse, G., Jones, M. C., Anthony, P. M., Iii, F. S. C., Finlay, J. C., Mack, M. C., Davydov, S., Frenzel, P., and Frohking, S.: A shift of thermokarst lakes from carbon sources to sinks during the Holocene epoch, *Nature*, 511, 452–456, <https://doi.org/10.1038/nature13560>, 2014.

Boike, J., Kattenstroth, B., Abramova, K., Bornemann, N., Chetverova, A., Fedorova, I., Fröb, K., Grigoriev, M., Grüber, M., Kutzbach, L., Langer, M., Minke, M., Muster, S., Piel, K., Pfeiffer, E.-M., Stouf, G., Westermann, S., Wischniewski, K., Wille, C., and Hubberten, H.-W.: Baseline characteristics of climate, permafrost and land cover from a new permafrost observatory

- 525 in the Lena River Delta, Siberia (1998–2011), *Biogeosciences*, 10, 2105–2128, <https://doi.org/10.5194/bg-10-2105-2013>, 2013.
- Callaghan, T. V., Bergholm, F., Christensen, T. R., Jonasson, C., Kokfelt, U., and Johansson, M.: A new climate era in the sub-Arctic: Accelerating climate changes and multiple impacts, *Geophysical Research Letters*, 37, <https://doi.org/10.1029/2009GL042064>, 2010.
- 530 Chasar, L. S., Chanton, J. P., Glaser, P. H., Siegel, D. I., and Rivers, J. S.: Radiocarbon and stable carbon isotopic evidence for transport and transformation of dissolved organic carbon, dissolved inorganic carbon, and CH₄ in a northern Minnesota peatland, *Global Biogeochemical Cycles*, 14, 1095–1108, <https://doi.org/10.1029/1999GB001221>, 2000.
- Conrad, R.: Control of microbial methane production in wetland rice fields, *Nutrient Cycling in Agroecosystems*, 64, 59–69, <https://doi.org/10.1023/A:1021178713988>, 2002.
- 535 Davidson, E. A. and Janssens, I. A.: Temperature sensitivity of soil carbon decomposition and feedbacks to climate change, *Nature*, 440, 165–173, <https://doi.org/10.1038/nature04514>, 2006.
- Dean, J. F., Middelburg, J. J., Röckmann, T., Aerts, R., Blauw, L. G., Egger, M., Jetten, M. S. M., de Jong, A. E. E., Meisel, O. H., Rasigraf, O., Slomp, C. P., in't Zandt, M. H., and Dolman, A. J.: Methane Feedbacks to the Global Climate System in a Warmer World, *Rev. Geophys.*, 56, 207–250, <https://doi.org/10.1002/2017RG000559>, 2018.
- 540 Deng, J., Gu, Y., Zhang, J., Xue, K., Qin, Y., Yuan, M., Yin, H., He, Z., Wu, L., Schuur, E. A. G., Tiedje, J. M., and Zhou, J.: Shifts of tundra bacterial and archaeal communities along a permafrost thaw gradient in Alaska, *Molecular Ecology*, 24, 222–234, <https://doi.org/10.1111/mec.13015>, 2015.
- Douglas, T. A., Turetsky, M. R., and Koven, C. D.: Increased rainfall stimulates permafrost thaw across a variety of Interior Alaskan boreal ecosystems, *npj Clim Atmos Sci*, 3, 1–7, <https://doi.org/10.1038/s41612-020-0130-4>, 2020.
- 545 Elder, C. D., Thompson, D. R., Thorpe, A. K., Hanke, P., Walter Anthony, K. M., and Miller, C. E.: Airborne Mapping Reveals Emergent Power Law of Arctic Methane Emissions, *Geophysical Research Letters*, 47, e2019GL085707, <https://doi.org/10.1029/2019GL085707>, 2020.
- Elderfield, H. and Schlesinger, W.: Biogeochemistry. An Analysis of Global Change, *Earth System Science and Global Change.*, *Geological Magazine*, 135, 819–842, <https://doi.org/10.1017/S0016756898231505>, 1998.
- 550 Ernakovich, J. G., Barabato, R. A., Rich, V. I., Schädel, C., Hewitt, R. E., Doherty, S. J., Whalen, E. D., Abbott, B. W., Barta, J., Biasi, C., Chabot, C. L., Hultman, J., Knoblauch, C., Vetter, M. C. Y. L., Lewis, M.-C., Liebner, S., Mackelprang, R., Onstott, T. C., Richter, A., Schütte, U. M. E., Siljanen, H. M. P., Taş, N., Timling, I., Vishnivetskaya, T. A., Waldrop, M. P., and Winkel, M.: Microbiome assembly in thawing permafrost and its feedbacks to climate, *Global Change Biology*, 28, 5007–5026, <https://doi.org/10.1111/gcb.16231>, 2022.
- 555 [Eskelinen, A., Stark, S., and Männistö, M.: Links between plant community composition, soil organic matter quality and microbial communities in contrasting tundra habitats, *Oecologia*, 161, 113–123, <https://doi.org/10.1007/s00442-009-1362-5>, 2009.](https://doi.org/10.1007/s00442-009-1362-5)
- Faucherre, S., Jørgensen, C. J., Blok, D., Weiss, N., Siewert, M. B., Bang-Andreasen, T., Hugelius, G., Kuhry, P., and Elberling, B.: Short and Long-Term Controls on Active Layer and Permafrost Carbon Turnover Across the Arctic, *Journal of Geophysical Research: Biogeosciences*, 123, 372–390, <https://doi.org/10.1002/2017JG004069>, 2018.
- 560 Fewster, R. E., Morris, P. J., Ivanovic, R. F., Swindles, G. T., Peregón, A. M., and Smith, C. J.: Imminent loss of climate space for permafrost peatlands in Europe and Western Siberia, *Nat. Clim. Chang.*, 12, 373–379, <https://doi.org/10.1038/s41558-022-01296-7>, 2022.
- Fuchs, M.: Soil organic carbon and nitrogen pools in thermokarst-affected permafrost terrain, phd, Universität Potsdam, 2019.
- 565 Ganzert, L., Jurgens, G., Münster, U., and Wagner, D.: Methanogenic communities in permafrost-affected soils of the Laptev Sea coast, Siberian Arctic, characterized by 16S rRNA gene fingerprints, *FEMS Microbiology Ecology*, 59, 476–488, <https://doi.org/10.1111/j.1574-6941.2006.00205.x>, 2007.
- Grigoriev, M. N.: Cryomorphogenesis in the Lena Delta. Yakutsk, Permafrost Institute Press, 176 pp, 1993.
- 570 Hales, B. A., Edwards, C., Ritchie, D. A., Hall, G., Pickup, R. W., and Saunders, J. R.: Isolation and identification of methanogen-specific DNA from blanket bog peat by PCR amplification and sequence analysis, *Applied and Environmental Microbiology*, <https://doi.org/10.1128/aem.62.2.668-675.1996>, 1996.

- Herbst, T.: Carbon Stocks and Potential Greenhouse Gas Release of Permafrost-affected Active Floodplains in the Lena River Delta, master, Faculty of Environment and Natural Resources, 73 pp., 2022.
- 575 Hinzman, L. D., Bettez, N. D., Bolton, W. R., Chapin, F. S., Dyurgerov, M. B., Fastie, C. L., Griffith, B., Hollister, R. D., Hope, A., Huntington, H. P., Jensen, A. M., Jia, G. J., Jorgenson, T., Kane, D. L., Klein, D. R., Kofinas, G., Lynch, A. H., Lloyd, A. H., McGuire, A. D., Nelson, F. E., Oechel, W. C., Osterkamp, T. E., Racine, C. H., Romanovsky, V. E., Stone, R. S., Stow, D. A., Sturm, M., Tweedie, C. E., Vourlitis, G. L., Walker, M. D., Walker, D. A., Webber, P. J., Welker, J. M., Winker, K. S., and Yoshikawa, K.: Evidence and Implications of Recent Climate Change in Northern Alaska and Other Arctic Regions, *Climatic Change*, 72, 251–298, <https://doi.org/10.1007/s10584-005-5352-2>, 2005.
- 580 Holm, S., Walz, J., Horn, F., Yang, S., Grigoriev, M. N., Wagner, D., Knoblauch, C., and Liebner, S.: Methanogenic response to long-term permafrost thaw is determined by paleoenvironment, *FEMS Microbiology Ecology*, 96, <https://doi.org/10.1093/femsec/fiaa021>, 2020.
- 585 Hugelius, G., Strauss, J., Zubrzycki, S., Harden, J. W., Schuur, E. a. G., Ping, C.-L., Schirrmeister, L., Grosse, G., Michaelson, G. J., Koven, C. D., O'Donnell, J. A., Elberling, B., Mishra, U., Camill, P., Yu, Z., Palmtag, J., and Kuhry, P.: Estimated stocks of circumpolar permafrost carbon with quantified uncertainty ranges and identified data gaps, *Biogeosciences*, 11, 6573–6593, <https://doi.org/10.5194/bg-11-6573-2014>, 2014a.
- Hugelius, G., Strauss, J., Zubrzycki, S., Harden, J. W., Schuur, E. a. G., Ping, C.-L., Schirrmeister, L., Grosse, G., Michaelson, G. J., Koven, C. D., O'Donnell, J. A., Elberling, B., Mishra, U., Camill, P., Yu, Z., Palmtag, J., and Kuhry, P.: Estimated stocks of circumpolar permafrost carbon with quantified uncertainty ranges and identified data gaps, *Biogeosciences*, 11, 6573–6593, <https://doi.org/10.5194/bg-11-6573-2014>, 2014b.
- 590 Huissteden, J. van, Maximov, T. C., and Dolman, A. J.: High methane flux from an arctic floodplain (Indigirka lowlands, eastern Siberia): methane flux arctic floodplain Siberia, *J. Geophys. Res.*, 110, n/a-n/a, <https://doi.org/10.1029/2005JG000010>, 2005.
- IPCC: IPCC, 2021: Climate Change 2021: The Physical Science Basis. Contribution of Working Group I to the Sixth Assessment Report of the Intergovernmental Panel on Climate Change, Cambridge University Press. In Press., 2021.
- 595 Jaatinen, K., Fritze, H., Laine, J., and Laiho, R.: Effects of short- and long-term water-level drawdown on the populations and activity of aerobic decomposers in a boreal peatland, *Global Change Biology*, 13, 491–510, <https://doi.org/10.1111/j.1365-2486.2006.01312.x>, 2007.
- 600 Jongejans, L. L., Liebner, S., Knoblauch, C., Mangelsdorf, K., Ulrich, M., Grosse, G., Tanski, G., Fedorov, A. N., Konstantinov, P. Ya., Windirsch, T., Wiedmann, J., and Strauss, J.: Greenhouse gas production and lipid biomarker distribution in Yedoma and Alas thermokarst lake sediments in Eastern Siberia, *Global Change Biology*, 27, 2822–2839, <https://doi.org/10.1111/gcb.15566>, 2021.
- Juncher Jørgensen, C., Lund Johansen, K. M., Westergaard-Nielsen, A., and Elberling, B.: Net regional methane sink in High Arctic soils of northeast Greenland, *Nature Geosci*, 8, 20–23, <https://doi.org/10.1038/ngeo2305>, 2015.
- 605 Keller, J. K. and Bridgman, S. D.: Pathways of anaerobic carbon cycling across an ombrotrophic-minerotrophic peatland gradient, *Limnology and Oceanography*, 52, 96–107, <https://doi.org/10.4319/lo.2007.52.1.0096>, 2007.
- Knoblauch, C., Beer, C., Sosnin, A., Wagner, D., and Pfeiffer, E.-M.: Predicting long-term carbon mineralization and trace gas production from thawing permafrost of Northeast Siberia, *Global Change Biology*, 19, 1160–1172, <https://doi.org/10.1111/gcb.12116>, 2013.
- 610 Knoblauch, C., Beer, C., Liebner, S., Grigoriev, M. N., and Pfeiffer, E.-M.: Methane production as key to the greenhouse gas budget of thawing permafrost, *Nature Climate Change*, 8, 309–312, <https://doi.org/10.1038/s41558-018-0095-z>, 2018.
- Koven, C. D., Ringeval, B., Friedlingstein, P., Ciais, P., Cadule, P., Khvorostyanov, D., Krinner, G., and Tarnocai, C.: Permafrost carbon-climate feedbacks accelerate global warming, *PNAS*, 108, 14769–14774, <https://doi.org/10.1073/pnas.1103910108>, 2011.
- 615 Kuhn, M. A., Thompson, L. M., Winder, J. C., Braga, L. P. P., Tanentzap, A. J., Bastviken, D., and Olefeldt, D.: Opposing Effects of Climate and Permafrost Thaw on CH₄ and CO₂ Emissions From Northern Lakes, *AGU Advances*, 2, e2021AV000515, <https://doi.org/10.1029/2021AV000515>, 2021.
- Kuhry, P., Bárta, J., Blok, D., Elberling, B., Faucherre, S., Hugelius, G., Jørgensen, C. J., Richter, A., Šantrůčková, H., and Weiss, N.: Lability classification of soil organic matter in the northern permafrost region, *Biogeosciences*, 17, 361–379, <https://doi.org/10.5194/bg-17-361-2020>, 2020.

- 620 Lara, M. J., Lin, D. H., Andresen, C., Loughheed, V. L., and Tweedie, C. E.: Nutrient Release From Permafrost Thaw Enhances CH₄ Emissions From Arctic Tundra Wetlands, *Journal of Geophysical Research: Biogeosciences*, 124, 1560–1573, <https://doi.org/10.1029/2018JG004641>, 2019.
- Lee, H., Schuur, E. A. G., Inglett, K. S., Lavoie, M., and Chanton, J. P.: The rate of permafrost carbon release under aerobic and anaerobic conditions and its potential effects on climate, *Global Change Biology*, 18, 515–527, <https://doi.org/10.1111/j.1365-2486.2011.02519.x>, 2012.
- 625 Li, F., Tianze, S., and Yahai, L.: Snapshot of methanogen sensitivity to temperature in Zoige wetland from Tibetan plateau, *Frontiers in Microbiology*, <https://doi.org/10.3389/fmicb.2015.00131>, 2015.
- Liebner, S., Ganzert, L., Kiss, A., Yang, S., Wagner, D., and Svenning, M. M.: Shifts in methanogenic community composition and methane fluxes along the degradation of discontinuous permafrost, *Frontiers in Microbiology*, 6, 2015.
- 630 Liljedahl, A. K., Boike, J., Daanen, R. P., Fedorov, A. N., Frost, G. V., Grosse, G., Hinzman, L. D., Iijima, Y., Jorgenson, J. C., Matveyeva, N., Necsoiu, M., Reynolds, M. K., Romanovsky, V. E., Schulla, J., Tape, K. D., Walker, D. A., Wilson, C. J., Yabuki, H., and Zona, D.: Pan-Arctic ice-wedge degradation in warming permafrost and its influence on tundra hydrology, *Nature Geosci*, 9, 312–318, <https://doi.org/10.1038/ngeo2674>, 2016.
- Mann, P. J., Sobczak, W. V., LaRue, M. M., Bulygina, E., Davydova, A., Vonk, J. E., Schade, J., Davydov, S., Zimov, N., 635 Holmes, R. M., and Spencer, R. G. M.: Evidence for key enzymatic controls on metabolism of Arctic river organic matter, *Global Change Biology*, 20, 1089–1100, <https://doi.org/10.1111/gcb.12416>, 2014.
- McCalley, C. K., Woodcroft, B. J., Hodgkins, S. B., Wehr, R. A., Kim, E.-H., Mondav, R., Crill, P. M., Chanton, J. P., Rich, V. I., Tyson, G. W., and Saleska, S. R.: Methane dynamics regulated by microbial community response to permafrost thaw, *Nature*, 514, 478–481, <https://doi.org/10.1038/nature13798>, 2014.
- 640 Megonigal, J. P. and Schlesinger, W. H.: Methane-limited methanotrophy in tidal freshwater swamps, *Global Biogeochemical Cycles*, 16, 35-1-35–10, <https://doi.org/10.1029/2001GB001594>, 2002.
- Meijboom, F. and Noordwijk, M. van: Rhizon soil solution samplers as artificial roots, in: *Root ecology and its practical application*, Verein für Wurzelforschung, A-9020 Klagenfurt Austria, 793–795, 1991.
- Morgenstern, A., Overduin, P. P., Günther, F., Stettner, S., Ramage, J., Schirrmeister, L., Grigoriev, M. N., and Grosse, G.: 645 Thermo-erosional valleys in Siberian ice-rich permafrost, *Permafrost and Periglacial Processes*, 32, 59–75, <https://doi.org/10.1002/ppp.2087>, 2021.
- Myers-Smith, I. H., Forbes, B. C., Wilmking, M., Hallinger, M., Lantz, T., Blok, D., Tape, K. D., Macias-Fauria, M., Sass-Klaassen, U., Lévesque, E., Boudreau, S., Ropars, P., Hermanutz, L., Trant, A., Collier, L. S., Wejers, S., Rozema, J., Rayback, S. A., Schmidt, N. M., Schaepman-Strub, G., Wipf, S., Rixen, C., Ménard, C. B., Venn, S., Goetz, S., Andreu-Hayles, L., 650 Elmendorf, S., Ravolainen, V., Welker, J., Grogan, P., Epstein, H. E., and Hik, D. S.: Shrub expansion in tundra ecosystems: dynamics, impacts and research priorities, *Environ. Res. Lett.*, 6, 045509, <https://doi.org/10.1088/1748-9326/6/4/045509>, 2011.
- Oblogov, G. E., Vasiliev, A. A., Streletskaia, I. D., Zadorozhnaya, N. A., Kuznetsova, A. O., Kanevskiy, M. Z., and Semenov, P. B.: Methane Content and Emission in the Permafrost Landscapes of Western Yamal, Russian Arctic, *Geosciences*, 10, 412, 655 <https://doi.org/10.3390/geosciences10100412>, 2020.
- Obu, J., Westermann, S., Bartsch, A., Berdnikov, N., Christiansen, H. H., Dashtseren, A., Delaloye, R., Elberling, B., Eitzelmüller, B., Kholodov, A., Khomutov, A., Kääh, A., Leibman, M. O., Lewkowicz, A. G., Panda, S. K., Romanovsky, V., Way, R. G., Westergaard-Nielsen, A., Wu, T., Yamkhin, J., and Zou, D.: Northern Hemisphere permafrost map based on TTOP modelling for 2000–2016 at 1 km² scale, *Earth-Science Reviews*, 193, 299–316, 660 <https://doi.org/10.1016/j.earscirev.2019.04.023>, 2019.
- Olefeldt, D., Turetsky, M. R., Crill, P. M., and McGuire, A. D.: Environmental and physical controls on northern terrestrial methane emissions across permafrost zones, *Global Change Biology*, 19, 589–603, <https://doi.org/10.1111/gcb.12071>, 2013.
- Osterkamp, T. E., Jorgenson, M. T., Schuur, E. a. G., Shur, Y. L., Kanevskiy, M. Z., Vogel, J. G., and Tumskey, V. E.: Physical and ecological changes associated with warming permafrost and thermokarst in Interior Alaska, *Permafrost and Periglacial Processes*, 20, 235–256, <https://doi.org/10.1002/ppp.656>, 2009.
- 665 Paul, S., Küsel, K., and Alewell, C.: Reduction processes in forest wetlands: Tracking down heterogeneity of source/sink functions with a combination of methods, *Soil Biology and Biochemistry*, 38, 1028–1039, <https://doi.org/10.1016/j.soilbio.2005.09.001>, 2006.

- 670 Pegoraro, E., Mauritz, M., Bracho, R., Ebert, C., Dijkstra, P., Hungate, B. A., Konstantinidis, K. T., Luo, Y., Schädel, C., Tiedje, J. M., Zhou, J., and Schuur, E. A. G.: Glucose addition increases the magnitude and decreases the age of soil respired carbon in a long-term permafrost incubation study, *Soil Biology and Biochemistry*, 129, 201–211, <https://doi.org/10.1016/j.soilbio.2018.10.009>, 2019.
- R Core Team: R: A Language and Environment for Statistical Computing, R Foundation for Statistical Computing, Vienna, Austria, 2021.
- 675 Rantanen, M., Karpechko, A. Y., Lipponen, A., Nordling, K., Hyvärinen, O., Ruosteenoja, K., Vihma, T., and Laaksonen, A.: The Arctic has warmed nearly four times faster than the globe since 1979, *Commun Earth Environ*, 3, 1–10, <https://doi.org/10.1038/s43247-022-00498-3>, 2022.
- Robertson, G. P., Coleman, D. C., Sollins, P., and Bledsoe, C. S.: *Standard Soil Methods for Long-term Ecological Research*, Oxford University Press, 481 pp., 1999.
- 680 Rößger, N., Sachs, T., Wille, C., Boike, J., and Kutzbach, L.: Seasonal increase of methane emissions linked to warming in Siberian tundra, *Nat. Clim. Chang.*, 12, 1031–1036, <https://doi.org/10.1038/s41558-022-01512-4>, 2022.
- Schädel, C., Schuur, E. A. G., Bracho, R., Elberling, B., Knoblauch, C., Lee, H., Luo, Y., Shaver, G. R., and Turetsky, M. R.: Circumpolar assessment of permafrost C quality and its vulnerability over time using long-term incubation data, *Glob Change Biol*, 20, 641–652, <https://doi.org/10.1111/gcb.12417>, 2014.
- 685 Schädel, C., Beem-Miller, J., Aziz Rad, M., Crow, S. E., Hicks Pries, C. E., Ernakovich, J., Hoyt, A. M., Plante, A., Stoner, S., Treat, C. C., and Sierra, C. A.: Decomposability of soil organic matter over time: the Soil Incubation Database (SIDb, version 1.0) and guidance for incubation procedures, *Earth System Science Data*, 12, 1511–1524, <https://doi.org/10.5194/essd-12-1511-2020>, 2020.
- 690 Schirrmeister, L., Kunitsky, V., Grosse, G., Wetterich, S., Meyer, H., Schwamborn, G., Babiy, O., Derevyagin, A., and Siegert, C.: Sedimentary characteristics and origin of the Late Pleistocene Ice Complex on north-east Siberian Arctic coastal lowlands and islands – A review, *Quaternary International*, 241, 3–25, <https://doi.org/10.1016/j.quaint.2010.04.004>, 2011.
- Schirrmeister, L., Froese, D., Tumskey, V., Grosse, G., and Wetterich, S.: PERMAFROST AND PERIGLACIAL FEATURES | Yedoma: Late Pleistocene Ice-Rich Syngenetic Permafrost of Beringia, in: *Encyclopedia of Quaternary Science*, Elsevier, 542–552, <https://doi.org/10.1016/B978-0-444-53643-3.00106-0>, 2013.
- 695 Schneider, J., Grosse, G., and Wagner, D.: Land cover classification of tundra environments in the Arctic Lena Delta based on Landsat 7 ETM+ data and its application for upscaling of methane emissions, *Remote Sensing of Environment*, 113, 380–391, <https://doi.org/10.1016/j.rse.2008.10.013>, 2009.
- 700 Schuur, E. a. G., McGuire, A. D., Schädel, C., Grosse, G., Harden, J. W., Hayes, D. J., Hugelius, G., Koven, C. D., Kuhry, P., Lawrence, D. M., Natali, S. M., Olefeldt, D., Romanovsky, V. E., Schaefer, K., Turetsky, M. R., Treat, C. C., and Vonk, J. E.: Climate change and the permafrost carbon feedback, *Nature*, 520, 171–179, <https://doi.org/10.1038/nature14338>, 2015.
- Schwamborn, G., Rachold, V., and Grigoriev, M. N.: Late Quaternary sedimentation history of the Lena Delta, *Quaternary International*, 89, 119–134, [https://doi.org/10.1016/S1040-6182\(01\)00084-2](https://doi.org/10.1016/S1040-6182(01)00084-2), 2002.
- 705 Serreze, M. C., Walsh, J. E., Chapin, F. S., Osterkamp, T., Dyurgerov, M., Romanovsky, V., Oechel, W. C., Morison, J., Zhang, T., and Barry, R. G.: Observational Evidence of Recent Change in the Northern High-Latitude Environment, *Climatic Change*, 46, 159–207, <https://doi.org/10.1023/A:1005504031923>, 2000.
- Siewert, M. B., Hugelius, G., Heim, B., and Faucherre, S.: Landscape controls and vertical variability of soil organic carbon storage in permafrost-affected soils of the Lena River Delta, *CATENA*, 147, 725–741, <https://doi.org/10.1016/j.catena.2016.07.048>, 2016.
- 710 Soil Survey Staff: *Keys to Soil Taxonomy*, 12th ed., Twelfth Edition, USDA-Natural Resources Conservation Service, Washington, DC, 360 pp., 2014.
- Spencer, R. G. M., Mann, P. J., Dittmar, T., Eglinton, T. I., McIntyre, C., Holmes, R. M., Zimov, N., and Stubbins, A.: Detecting the signature of permafrost thaw in Arctic rivers, *Geophysical Research Letters*, 42, 2830–2835, <https://doi.org/10.1002/2015GL063498>, 2015.
- 715 Strauss, J., Schirrmeister, L., Grosse, G., Wetterich, S., Ulrich, M., Herzschuh, U., and Hubberten, H.-W.: The deep permafrost carbon pool of the Yedoma region in Siberia and Alaska, *Geophysical Research Letters*, 40, 6165–6170, <https://doi.org/10.1002/2013GL058088>, 2013a.

- Strauss, J., Schirmer, L., Grosse, G., Wetterich, S., Ulrich, M., Herzsuh, U., and Hubberten, H.-W.: The deep permafrost carbon pool of the Yedoma region in Siberia and Alaska, *Geophysical Research Letters*, 40, 6165–6170, <https://doi.org/10.1002/2013GL058088>, 2013b.
- 720 Symons, G. E. and Buswell, A. M.: The methane fermentation of carbohydrates., vol. 55, *J. Am. Chem. Soc.*, 2028–2036, 1993.
- Tabari, H.: Climate change impact on flood and extreme precipitation increases with water availability, *Sci Rep*, 10, 13768, <https://doi.org/10.1038/s41598-020-70816-2>, 2020.
- Thauer, R. K.: Biochemistry of methanogenesis: a tribute to Marjory Stephenson:1998 Marjory Stephenson Prize Lecture, *Microbiology*, 144, 2377–2406, <https://doi.org/10.1099/00221287-144-9-2377>, 1998.
- 725 Theisen, A. R. and Murrell, J. C.: Facultative Methanotrophs Revisited, *Journal of Bacteriology*, 187, 4303–4305, <https://doi.org/10.1128/JB.187.13.4303-4305.2005>, 2005.
- Treat, C. C., Natali, S. M., Ernakovich, J., Iversen, C. M., Lupascu, M., McGuire, A. D., Norby, R. J., Roy Chowdhury, T., Richter, A., Šantrůčková, H., Schädel, C., Schuur, E. A. G., Sloan, V. L., Turetsky, M. R., and Waldrop, M. P.: A pan-Arctic synthesis of CH₄ and CO₂ production from anoxic soil incubations, *Glob Change Biol*, 21, 2787–2803, <https://doi.org/10.1111/gcb.12875>, 2015.
- 730 Treat, C. C., Marushchak, M. E., Voigt, C., Zhang, Y., Tan, Z., Zhuang, Q., Virtanen, T. A., Räsänen, A., Biasi, C., Hugelius, G., Kaverin, D., Miller, P. A., Stendel, M., Romanovsky, V., Rivkin, F., Martikainen, P. J., and Shurpali, N. J.: Tundra landscape heterogeneity, not interannual variability, controls the decadal regional carbon balance in the Western Russian Arctic, *Global Change Biology*, 24, 5188–5204, <https://doi.org/10.1111/gcb.14421>, [2018b](https://doi.org/10.1111/gcb.14421)2018.
- 735 Turetsky, M. R., Abbott, B. W., Jones, M. C., Walter Anthony, K., Olefeldt, D., Schuur, E. A. G., Koven, C., McGuire, A. D., Grosse, G., Kuhry, P., Hugelius, G., Lawrence, D. M., Gibson, C., and Sannel, A. B. K.: Permafrost collapse is accelerating carbon release, *Nature*, 569, 32–34, <https://doi.org/10.1038/d41586-019-01313-4>, 2019.
- Wagner, D., Gattinger, A., Embacher, A., Pfeiffer, E.-M., Schloter, M., and Lipski, A.: Methanogenic activity and biomass in Holocene permafrost deposits of the Lena Delta, Siberian Arctic and its implication for the global methane budget, *Global Change Biology*, 13, 1089–1099, <https://doi.org/10.1111/j.1365-2486.2007.01331.x>, 2007.
- 740 Waldrop, M. P., Wickland, K. P., White Iii, R., Berhe, A. A., Harden, J. W., and Romanovsky, V. E.: Molecular investigations into a globally important carbon pool: permafrost-protected carbon in Alaskan soils, *Global Change Biology*, 16, 2543–2554, <https://doi.org/10.1111/j.1365-2486.2009.02141.x>, 2010.
- 745 Walz, J., Knoblauch, C., Böhme, L., and Pfeiffer, E.-M.: Regulation of soil organic matter decomposition in permafrost-affected Siberian tundra soils - Impact of oxygen availability, freezing and thawing, temperature, and labile organic matter, *Soil Biology and Biochemistry*, 110, 34–43, <https://doi.org/10.1016/j.soilbio.2017.03.001>, 2017.
- Walg, J., Knoblauch, C., Tigges, R., Opel, T., Schirmer, L., and Pfeiffer, E.-M.: Greenhouse gas production in degrading ice-rich permafrost deposits in northeastern Siberia, *Biogeosciences*, 15, 5423–5436, <https://doi.org/10.5194/bg-15-5423-2018>, 2018.
- 750 Wang, P., Huang, Q., Tang, Q., Chen, X., Yu, J., Pozdniakov, S. P., and Wang, T.: Increasing annual and extreme precipitation in permafrost-dominated Siberia during 1959–2018, *Journal of Hydrology*, 603, 126865, <https://doi.org/10.1016/j.jhydrol.2021.126865>, 2021.
- Washburn, A. L.: *Periglacial processes and environment.*, St. Martin's Press, New York, 1973.
- 755 Westermann, P.: Temperature regulation of methanogenesis in wetlands, *Chemosphere*, 26, 321–328, [https://doi.org/10.1016/0045-6535\(93\)90428-8](https://doi.org/10.1016/0045-6535(93)90428-8), 1993.
- Yavitt, J. B., Williams, C. J., and Wieder, R. K.: Production of methane and carbon dioxide in peatland ecosystems across North America: Effects of temperature, aeration, and organic chemistry of peat, *Geomicrobiology Journal*, 14, 299–316, <https://doi.org/10.1080/01490459709378054>, 1997.
- 760 Yavitt, J. B., Basiliko, N., Turetsky, M. R., and Hay, A. G.: Methanogenesis and Methanogen Diversity in Three Peatland Types of the Discontinuous Permafrost Zone, Boreal Western Continental Canada, *Geomicrobiology Journal*, 23, 641–651, <https://doi.org/10.1080/01490450600964482>, 2006.

Zhu, X., Wu, T., Li, R., Xie, C., Hu, G., Qin, Y., Wang, W., Hao, J., Yang, S., Ni, J., and Yang, C.: Impacts of Summer Extreme Precipitation Events on the Hydrothermal Dynamics of the Active Layer in the Tanggula Permafrost Region on the Qinghai-Tibetan Plateau, *Journal of Geophysical Research: Atmospheres*, 122, 11,549-11,567, <https://doi.org/10.1002/2017JD026736>, 2017.